RERTR 2014 - 35TH INTERNATIONAL MEETING ON
REDUCED ENRICHMENT FOR RESEARCH AND TEST REACTORS

OCTOBER 12-16, 2014
IAEA VIENNA INTERNATIONAL CENTER
VIENNA, AUSTRIA

Accident Analyses for the Conversion of the University of Missouri Research Reactor from Highly-Enriched to Low-Enriched Uranium

L. Foyto, K. Kutikkad, J. C. McKibben and N. Peters
University of Missouri-Columbia Research Reactor
1513 Research Park Drive, Columbia, Missouri 65211 – USA

W. Cowherd
Nuclear Engineering Program – College of Engineering
University of Missouri-Columbia
Columbia, Missouri 65211 – USA

E. Feldman, E. Wilson, J. Stillman and J. Stevens
Argonne National Laboratory
9700 South Cass Avenue, Argonne, Illinois 60439 – USA

ABSTRACT

The University of Missouri Research Reactor (MURR®) is one of five U.S. high performance research and test reactors that are actively collaborating with the Global Threat Reduction Initiative (GTRI) Reduced Enrichment for Research and Test Reactors (RERTR) Program to find a suitable low-enriched uranium (LEU) fuel replacement for the currently required highly-enriched uranium (HEU) fuel. Analyses of accident scenarios for a proposed core loaded with U-10Mo monolithic LEU fuel have been completed. The models include both fresh and irradiated fuel assemblies. Furthermore, a series of branch cases to evaluate the impact of the uncertainties in core operating conditions or fuel thermo-physical properties that may affect the severity of the accidents are considered. Results for a positive reactivity insertion accident (RIA), a loss of coolant accident (LOCA) and the maximum hypothetical accident (MHA) are presented in this paper. All accident scenarios demonstrate an acceptable margin to potential fuel damage, or acceptable dose consequences in the case of the MHA.

1. Introduction

Because of its compact core design (33 liters), which requires a very high loading density of ^{235}U, the University of Missouri Research Reactor (MURR®) could not perform its mission with any previously qualified low-enriched uranium (LEU) fuels. However, in 2006 with the prospect of the Global Threat Reduction Initiative (GTRI) Fuel Development (FD) Program validating the performance of U-10Mo monolithic LEU foil fuels, MURR began actively collaborating with the GTRI Conversion Program, and four other U.S. high-performance research and test reactors that use highly-enriched uranium (HEU) fuel, to find a suitable LEU fuel replacement. It was concluded that the proposed LEU fuel assembly design, in conjunction with an increase in power level from 10 to 12 MW_{th}, will (1) maintain safety margins during steady-state operation, (2) allow operating fuel cycle lengths to be maintained for efficient and effective use of the facility, and (3) preserve an acceptable level and spectrum of key neutron fluxes to meet the scientific mission of the facility. This paper provides the results for accident scenarios in support of converting MURR from U-Al_x aluminide dispersion HEU fuel to U-10Mo monolithic LEU fuel.

2. Thermo-Physical Properties of HEU and LEU Fuel

The thermo-physical properties of the materials of construction for the MURR fuel plates are needed for proper modeling of heat conduction and temperatures during accident analyses. A search of the published literature and available technical reports was conducted. A summary of the data used in modeling the positive Reactivity Insertion Accident (RIA) and Loss of Coolant Accident (LOCA) are reported in this section.

The value of thermal conductivity for the fresh HEU fuel meat can be obtained from Reference 1. The data indicate that the thermal conductivity for the fresh U-Al_x is in the range of 40 to 45 W/m-C. A lower bound value for the thermal conductivity of high-burnup MURR HEU fuel is 30 W/m-C [2]. Consequently, the U-Al_x thermal conductivity was assumed to reduce linearly from 40 W/m-C for fresh HEU fuel to 30 W/m-C for the maximum burnup HEU fuel (average element burnup of 150 MWd). The U-Al_x thermal conductivity does not vary with temperature. Reference 1 provides the heat capacity of U-Al_x fuel as 0.387 + 0.00022 T in J/g-C, where T is in K and the applicable range is 20 to 600 °C.

Reference 3 provides a summary of measurements for the thermal conductivity of unirradiated U-10Mo from a number of experimenters. The Burkes' measurements based on a laser flash thermal diffusivity technique are considered the most accurate and were fit by a linear function with temperature. Reference 4 reported the results of measurements of thermal conductivity for samples of irradiated U-10Mo with fission densities ranging from 2.9 to 4.1×10^{21} fissions/cm^3 and temperatures of 50, 150, and 300 °C. These data were fit as a function of fission density and temperature. Table 1 summarizes the fuel element burnup, peak fission density in plate 23 (the location of peak heat flux in all LEU elements), and associated thermal conductivity for fuel elements at various burnups that will be modeled in the accident analyses. Compared to the unirradiated data, the thermal conductivity decreases by about 35% from beginning-of-life (BOL) to end-of-life (EOL) (2.6×10^{21} fissions/cm^3). This will be an important phenomenon to model in the accident analyses to accurately evaluate the fuel temperatures of BOL, middle-of-life (MOL), and EOL fuel plates.

Table 1 – Thermal Conductivity of U-10Mo in Unirradiated and Irradiated LEU Fuel Elements.

Element	**Element Burnup (MWd)**	**Peak Fission Density in Plate 23 (fissions/cm^3)[a]**	**Thermal Conductivity, κ (W/m-C), in range from 50 to 300 °C**	**Minimum ratio of $\kappa/\kappa_{unirradiated}$[b]**
Fresh (Unirradiated U-10Mo)	0	0.0	16.37 (50 °C) to 24.09 (300 °C)[c]	
Avg. Element in Reference Mixed-Burnup Core[d]	85.9	1.25×10^{21}	12.67 (50 °C) to 19.20 (300 °C)[e]	0.77
Middle-of-Life (MOL)	77	1.15×10^{21}	12.82 (50 °C) to 19.46 (300 °C)[e]	0.78
	96	1.40×10^{21}	12.45 (50 °C) to 18.81 (300 °C)[e]	0.75
End-of-Life (EOL)	180	2.60×10^{21}	10.68 (50 °C) to 15.68 (300 °C)[e]	0.65

[a] Assume local fission density in LEU elements is linearly proportional to the fuel element burnup. The peak local fission density in plate 23 was calculated to be 2.6×10^{21} fissions/cm^3 for a discharged LEU element at 180 MWd in a MURR fuel cycle simulation performed in the steady-state technical basis evaluation [6].

[b] Minimum ratio over temperature range 50 - 300 °C.

[c] Thermal conductivity for unirradiated U-10Mo evaluated from fit of Burkes 2010 data [3].

[d] Average burnup of all elements in reference mixed-burnup core derived in Reference 6.

[e] Thermal conductivity for irradiated U-10Mo evaluated from fit of data in Reference 4.

Reference 4 states that "the specific heat capacity of the U-10Mo fuel is not significantly dependent on burnup." Consequently, the correlation for the volumetric heat capacity of U-10Mo derived from Reference 5 will be used for all unirradiated and irradiated fuel plates in the accident analyses.

For the structural materials in the MURR, thermo-physical property data from References 7 and 8 were used for the 6061-T6 aluminum alloy (fuel clad, island tube, piping) and the LEU fuel plate zirconium interlayer, respectively. For the oxide layer, Reference 9 provided the thermal conductivity of the material as $\kappa_{oxide} = 2.25$ W/m-C. No data was located for the volumetric heat capacity of the oxide, but a very low (conservative) value of 1.0 J/m^3-C was selected for the RIA and LOCA analyses. For all practical purposes, this value is essentially zero, but avoids a potential division-by-zero error in the simulation codes.

3. Reactivity Insertion Accident

3.1 Introduction

Insertion of uncontrolled and/or unanticipated positive reactivity to either a critical reactor or during a reactor startup is one of the nine (9) postulated accident-initiating scenarios required to be analyzed for potential radiological consequence per NUREG-1537 guidelines [10]. The exact mechanisms or events that could cause these reactivity insertions can vary, but could include an inadvertent rapid insertion or removal of an experiment from the center test hole, reactor or equipment malfunction, or operator error.

3.2 Modeling

All the analyses in this section were performed using the PARET/ANL code [11]. PARET/ANL is a 1-dimensional reactor transient analysis code that models plate, pin and nested tube fuel geometries. The collection of fuel meat, clad, and associated coolant is called a "channel" in PARET/ANL. An average channel is typically used to represent the core and bulk reactivity feedback effects from the transient, while one or more "peak" channels are used to represent those components (e.g., a fuel plate) which are expected to reach the highest temperature as a result of the transient. There is no heat transfer between the channels in PARET/ANL, so the hottest channels are conservatively modeled.

The reactivity feedback coefficients from fuel and coolant temperature changes and reactor kinetics parameters [effective delayed neutron fraction (β_{eff}) and neutron lifetime (Λ)] were calculated for the MURR core loaded with HEU or LEU fuel using an MCNP5 [12] core model for all fresh and reference mixed burnup cores. Reactor safety systems are also available to terminate any transient. When any one of the various reactor trip settings is reached, a scram signal is sent and four BORAL® shim control blades are dropped into a water-filled gap between the outer reactor pressure vessel and the beryllium reflector to terminate the transient. There is a short delay time of approximately 150 milliseconds from the time the scram signal is sent to the start of blade inward motion. The reactivity feedback parameters and control blade worth data are summarized in Reference 13.

In the current analysis, up to four fuel plate/coolant channels were modeled in PARET/ANL to represent the MURR core plus the fuel plates most likely to have peak fuel temperatures. The channels to be modeled will be 1) an average channel representing the core, 2) a BOL (unirradiated) fuel plate with the peak heat flux of all fresh fuel plates in the core, 3) an EOL plate with the peak heat flux of all EOL plates in the core, and 4) a MOL plate with the peak heat flux of all MOL plates in the core. The plate with the peak heat flux in the HEU cores is plate 1, while the plate with the peak heat flux in the LEU cores is plate 23. Appropriate degradation of the U-10Mo thermal conductivity with fuel burnup, the formation of an oxide layer on irradiated fuel plates, and reduction of the coolant channel due to oxide growth, fuel swelling, and fuel creep will be modeled in the MOL, EOL, and average fuel channels.

The thickness of the oxide layer on the irradiated fuel plates was estimated from a version of the Griess correlation [9] which was modified to take into account the specific operating conditions

of the MURR based on oxide thickness measurements of plate 24 of HEU fuel elements [14]. This correlation predicts an oxide thickness of 0.54 mil (0.00054 inches) for an HEU fuel plate 1 under nominal operating conditions and at an EOL element burnup of 150 MWd. For the LEU fuel plate 23 under nominal operating conditions and in an EOL element at 180 MWd, the oxide layer thickness is predicted to be 0.93 mil (0.00093 inches). During irradiation, the coolant channel between the fuel plates will become constricted relative to the fresh element coolant channel due to oxide growth, fuel swelling, and irradiation-induced fuel creep. For the HEU fuel, the acceptance criteria for the elements during irradiation limits this constriction to a maximum of 10 mil. For the LEU fuel, it was determined that the total coolant channel restriction for channels bounded by two fuel plates will be no more than 8 mil due to these effects [14]. The channel restriction is assumed to increase linearly, reaching 10 mil in the HEU element at the expected element discharge burnup of 150 MWd, or 8 mil in the LEU element at the expected element discharge burnup of 180 MWd.

Detailed, 3-dimensional power density distributions in MURR cores loaded with HEU or LEU fuel were calculated using MCNP5 as part of the steady-state safety basis for a number of reference cores [6]. For the peak BOL, MOL, and EOL channels in the PARET/ANL models, the axial heat source description can be calculated using the power density in the plate and azimuthal strip in the core that generates the highest local heat flux, while for the average channel the axial heat source description can be calculated using the average power density of all plates in the core. The heat source description takes into account that a fraction of the energy generated from fission events is deposited outside the primary coolant system. Based on calculations performed at MURR, these fractions amount to 6.0% and 3.6%, respectively, for the HEU and LEU cores [19].

The peak heat flux in the HEU elements in the reference cores always occurs in plate 1, while for the LEU reference cores the peak heat flux always occurs in plate 23. These plates are cooled by water flowing along both sides of the plate, but the coolant channel properties on each side of the plate are different. Specifically, the coolant channels on the concave (inboard) and convex (outboard) sides of these fuel plates have different thicknesses. Also, the coolant on the concave side HEU plate 1 (adjacent to the inner pressure vessel wall) and the convex side of LEU plate 23 (adjacent to the outer pressure vessel wall) is heated by only one fuel plate. Consequently, the side of the fuel plate hat is adjacent to the pressure vessels is better cooled and most of the heat generated in these plates will conduct out of the cooler side of the plate. PLTEMP [15] models for each of the reference cores under the assumed steady-state conditions that will exist prior to the RIA were used to evaluate the "power split" between the two curved sides of these fuel plates. For the HEU elements, the power split is about 54.5% / 45.5% for the inboard/outboard sides of plate 1. The power split for the inboard/outboard sides of LEU fuel plate 23 is 48.3% / 51.7%; the power split is slightly less for the LEU plate 23 because the difference in the coolant channel dimensions between the two sides of the limiting LEU plate are not as great as they are for the limiting HEU plate. These power splits were applied when calculating the heat source description for the PARET/ANL model for those channels with the peak heat flux.

Table 2 summarizes the operating conditions for MURR for nominal full-power operations and the limiting safety system settings (LSSSs) for steady-state operations. The MURR typically

operates at or near the nominal conditions listed in the table, but there is a typical range for these operating parameters, as shown in the table. For the initial steady-state conditions for the RIAs, values for the coolant flow rate, pressure, and coolant inlet temperature that are at the limits of the typical operating range were chosen that will yield conservative results for the consequences of the accidents. Thus, the core flow rate and pressurizer pressure that are at the lower end of the typical operating band and the coolant inlet temperature that is at the upper end of the typical operating band were selected.

The preceding discussion provides the steady-state conditions that were assumed for a "base case" for the evaluation of each of the RIAs. No hot channel factors were applied in the RIA analyses. However, a series of branch cases were performed to cover potential non-conservative variations of thermo-physical properties or core operating conditions that may affect the severity of the accidents. These variations will be discussed along with the results in the next section.

Table 2 – MURR Operating Conditions.

Parameter	**Nominal (Range)**	**LSSS**	**Reactivity Insertion Accident Analyses**
Reactor Power, MW	HEU: 10 LEU: 12	HEU: 12.5[1] LEU: 15.0[1]	HEU: 10 LEU: 12
Core Power, MW (Primary Coolant System)	HEU: 9.40[2] LEU: 11.57[2]	HEU: 11.75[2] LEU: 14.46[2]	HEU: 9.40[2] LEU: 11.57[2]
Primary Coolant Flow Rate, gpm	3,800 (3,700 to 3,850)	HEU: 3,200 LEU: 3,300[3]	3,700
Core Inlet Pressure, psia	HEU: 68.4[4] LEU: 69.1[4]	HEU: 63.2[4] LEU: 63.0[4]	HEU: 59.3[4] LEU: 59.9[4]
Coolant Inlet Temperature, ^{o}F	120 (118 – 125)	HEU: 155 LEU: 145[3]	125

[1] 125% of full core power.

[2] HEU core power is 94.0% of reactor power (6.0% of power deposited outside primary coolant system). LEU core power is 96.4% of reactor power, (3.6% of power deposited outside primary coolant system) [19].

[3] LSSS conditions for primary coolant flow rate and core inlet temperature for LEU core determined in steady-state safety basis [2].

[4] Pressure calculated just inside the entrance to the coolant channels between the MURR fuel plates by spreadsheet model.

3.3 Results

Three different types of accidents that insert reactivity up to the limits of the MURR Technical Specifications (TS) were evaluated. Of these accidents, the step insertion of 0.6% $\Delta k/k$ was found to result in the highest fuel meat temperature. The results of this accident will be presented below.

The consequences of the step RIA in two different reference core states were evaluated for both HEU and LEU fuel. The so-called 1B1 (HEU) and 5B1 (LEU) all-fresh fuel core configurations had the highest local heat flux of a set of 24 core configurations considered as part of the steady-state safety basis [6]. However, these are core states that the reactor will rarely, if ever,

experience. The typical condition for the MURR is represented by the so-called 3A (HEU) and 7A (LEU) cores that are loaded with fuel elements that have a mixture of burnups.

Results for the 0.6% Δk/k step RIA in the cores loaded with HEU fuel are presented in Table 3. The base case assumes the initial steady-state conditions summarized in Table 2. These conditions are at the limits of the normal operating band for MURR that would provide conservative results for the accident. The step insertion of 0.6% Δk/k reactivity in the critical, steady-state core results in a sharp reactor power rise from 10 MW to nearly 34.3 MW in both the all-fresh and mixed-burnup reference cores before the transient is curtailed by negative reactivity feedback effects from changes in the coolant conditions (density and temperature). The transient is terminated by reactor scram at 0.152 seconds after the reactivity insertion. The peak fuel meat temperature reached during the accident in the all fresh core is 212.5 °C. However, this is for a core state that is not used for reactor operations (all fresh fuel, empty flux trap, skewed and highly depleted control blades). For the reference mixed-burnup core that is typical for MURR operations, the peak HEU fuel temperature reached in the accident is predicted to be 194.0 °C in a fresh plate 1 in element position 5. This is well below the measured U-Al_x blister threshold temperature 480 °C [16]. The peak fuel temperatures in the MOL and EOL plates in this core are predicted to be 188.8 °C and 168.6 °C, respectively.

Table 3 – Peak Reactor Power and Peak Fuel Temperature for 0.6% Δk/k Step Insertion of Reactivity in HEU Reference Cores.

		Reactor Power, MW		Peak Fuel Temperature, °C (Plate)		*Effect of branch case on peak fuel temperature relative to base case for Core 3A*, °C
		All Fresh Core (1B1)	Mixed Burnup Core (3A)	All Fresh Core (1B1)	Mixed Burnup Core (3A)	
Base Case (T_{inlet} = 125 °F, Flow = 3700 gpm, Pressurizer pressure = 74.3 psia, Pressurizer level = -7 inches)		34.25	34.27	212.5 (BOL)	**194.0 (BOL)**	
Branch02	Increase oxide layer thickness by 18%		34.34		194.5 (BOL)	*+0.4 Minimal*
Branch03b	No coolant channel restriction with burnup		34.53		203.0 (BOL)	*+9.0 More severe*
Branch04a	T_{inlet} = 155 °F (LSSS temp.)	33.56	33.61	212.9 (BOL)	199.7 (BOL)	*+5.6 More severe*
Branch04b	Flow = 3200 gpm (LSSS flow)	34.35	34.35	216.2 (BOL)	203.2 (BOL)	*+9.2 More severe*
Branch05	Mode II LSSS Operating Conditions	18.26	18.23	200.5 (BOL)	188.7 (BOL)	*-5.3 Less severe*
Branch06b	$t_{insertion}$ = 0.1 s	34.25	34.27	212.5 (BOL)	194.0 (BOL)	*0.0 Minimal*

Several branch cases were also run to estimate the effect of potential non-conservative variations of the core operating conditions on the severity of the accident in the HEU core. In the Branch02 case, the oxide layer thickness on the MOL and EOL plates was increased by 18% relative to the base case. An oxide layer thickness of 0.54 mil on an EOL plate in the plate 1 position had previously been estimated from a modified Griess correlation [14] based on fuel elements in a core operating at nominal conditions (see Table 2). However, if the MURR consistently operated at the limits of the operating band assumed for the RIAs, the oxide layer thickness on an EOL plate in the plate 1 position is estimated to be 0.63 mil (18% thicker). The increased oxide thickness results in a 2.6 °C increase in the peak fuel temperature in the EOL plate (up to 171.2 °C from 168.6 °C in the base case), but there is only a marginal effect on the peak fuel temperature in the BOL plate in the core.

In the base case, the coolant channel restriction at EOL due to irradiation effects was set at the MURR acceptance criteria of ≤ 10 mil. In the Branch03b case it was assumed that coolant channels remain at their nominal gap (i.e., there is no channel restriction with burnup). Under these conditions the peak power is 190 kW higher relative to the base case and the peak fuel temperature reached in the BOL plate during the accident is 9.0 °C higher. Without the reduction of the coolant channel gap from burnup-related effects, the EOL channel receives a greater fraction of the coolant flow rate than in the base case, reducing the coolant flow rate in the BOL channel. This effect, along with the increased reactor power level reached in the transient, leads to the higher fuel temperature.

Three branch cases based on the LSSSs were evaluated. In the Branch04a and Branch04b cases, the coolant inlet temperature and coolant flow rate are set at the LSSS values, respectively. Initiating the accident from these operating conditions results in an increase in the peak fuel temperature relative to the base case. Using the inlet temperature LSSS gives a 5.6 °C rise in the fuel temperature, while the LSSS flow increases the peak fuel temperature 9.2 °C. Case Branch05 shows the effect of the step RIA in a core operating in Mode II LSSS conditions [half nominal power, T_{inlet} = 155 °F (68.3 °C), single coolant loop for total flow of 1600 gpm]. The peak fuel temperature is 5.3 °C lower in this case.

The last branch case evaluated the impact of the insertion time for the 0.6% Δk/k reactivity in the accident. The time needed to eject the unsecured experiments from the core was conservatively set to 10 μs in the base case. In the Branch06b case the ejection time was increased to 0.1 seconds, which is a more realistic time. This adjustment had a negligible effect on the accident consequence.

The modeling variations in the Branch03b, Branch04a, and Branch04b cases (shaded rows in Table 3) are each within the allowed operations of the MURR. Each of these cases resulted in an increase in the peak fuel temperature predicted for the 0.6% Δk/k step RIA. Among all of the cases considered, the peak U-AL_x fuel temperature was 203.2 ^{o}C for the 0.6% Δk/k step RIA.

Results for the 0.6% Δk/k step RIA in the cores loaded with LEU fuel are presented in Table 4. The base case assumed the same operating conditions as for the HEU accident analyses. The step insertion of 0.6% Δk/k reactivity in the critical, steady-state core results in a sharp reactor power rise from 12 MW to about 42 MW in both the all-fresh and mixed-burnup reference cores

before the transient is curtailed by negative reactivity feedback effects from changes in the fuel temperature and coolant conditions (density and temperature). The transient is terminated by reactor scram at 0.152 seconds after the reactivity insertion. The peak fuel meat temperature reached during the accident in the all fresh Core 5B1 is 251.0 °C. This is a core state that is not expected to be used for reactor operations. For the expected reference mixed-burnup core that is typical for MURR operations (Core 7A), the peak LEU fuel temperature reached in the accident is predicted to be 264.0 °C in an MOL plate 23 in element position 6.

Table 4 – Peak Reactor Power and Peak Fuel Temperature for 0.6% Δk/k Step Insertion of Reactivity in LEU Reference Cores.

		Reactor Power, MW		Peak Fuel Temperature, °C (Plate)		*Effect of branch case on peak fuel temperature relative to base case for Core 7A*, °C
		All Fresh Core (5B1)	Mixed Burnup Core (7A)	All Fresh Core (5B1)	Mixed Burnup Core (7A)	
Base Case (T_{in} = 125 °F, Flow = 3700 gpm, Pressurizer pressure = 74.3 psia, Pressurizer level = -7 inches)		41.82	42.00	251.0 (BOL)	**264.0 (MOL)**	
Branch01	Decrease $\kappa_{U10\text{-}Mo}$ by 20%	41.83	42.00	259.0 (BOL)	270.9 (MOL)	*+6.9 More severe*
Branch02	Increase oxide layer thickness by 23%		42.07		270.8 (MOL)	*+6.8 More severe*
Branch03b	No coolant channel restriction with burnup		42.12		266.5 (MOL)	*+2.5 More severe*
Branch04a	T_{inlet} = 145 °F (LSSS temp.)	41.38	41.61	250.8 (BOL)	263.7 (MOL)	*-0.3 Minimal*
Branch04b	Flow = 3300 gpm (LSSS flow)	41.91	42.05	253.9 (BOL)	267.9 (MOL)	*+3.9 More severe*
Branch05	Mode II LSSS Operating Conditions	22.60	22.64	222.6 (BOL)	227.6 (MOL)	*-36.4 Less severe*
Branch06b	$t_{insertion}$ = 0.1 s	38.32	38.48	248.5 (BOL)	263.1 (MOL)	*-0.9 Less severe*

Several branch cases were run to estimate the effect of potential non-conservative variations of the thermo-physical properties or core operating conditions on the severity of the accident. In the Branch01 case, the thermal conductivity of the U-10Mo was reduced by 20% from that used in the base case. This takes into account the experimental uncertainty in the U-10Mo thermal conductivity measurements conducted in Reference 4. The predicted peak reactor power from the reactivity insertion is not affected by this modeling change. However, the predicted peak fuel temperatures are higher because of the lower thermal conductivity. The peak fuel temperature in the limiting MOL fuel plate in Core 7A is 6.9 °C higher relative to the base case.

In the Branch02 case, the oxide layer thickness on the MOL and EOL plates was increased by 23% relative to the base case to account for the impact of core operating conditions on the oxide thickness. An oxide layer thickness of 0.93 mil on the concave surface of an EOL plate in the plate 23 position had previously been estimated from a modified Griess correlation [14] based on fuel elements in a core operating at nominal conditions. As was done for the HEU accident analyses, if the MURR consistently operated at the limits of the operating band assumed for the reactivity insertion accidents, the oxide layer thickness on the fuel plates was computed to be 23% thicker. The increased oxide thickness results in a 6.8 °C increase in the peak fuel temperature in the limiting MOL plate.

In the base case, the coolant channel restriction at EOL due to irradiation effects was set at the anticipated MURR acceptance criteria for LEU elements of ≤ 8 mil. In the Branch03b case it was assumed that coolant channels remain at their nominal gap (i.e., there is no channel restriction with burnup). Under these conditions the peak power is 120 kW higher relative to the base case and the peak fuel temperature reached in the limiting MOL plate during the accident is 2.5 °C higher.

Three branch cases based on the LSSSs were evaluated. In the Branch04a and Branch04b cases, the coolant inlet temperature and coolant flow rate are set at the LSSS values, respectively. Initiating the accident from these operating conditions results in an increase in the peak fuel temperature relative to the base case. Using the inlet temperature LSSS gives a 0.3 °C decrease in the fuel temperature. Although the steady-state fuel temperature is higher because the coolant inlet temperature is increased by 11.1 °C, the peak power reached during the transient is 390 kW lower so that there is less energy deposition in the core due to the transient. Initiating the transient from the LSSS flow rate increases the peak fuel temperature 3.9 °C. Case Branch05 shows the effect of the step RIA in a core operating in Mode II LSSS conditions [half nominal power, T_{inlet} = 145 °F (68.3 °C), single coolant loop for total flow of 1650 gpm]. The peak fuel temperature is 36.4 °C lower in this case.

The last branch case evaluated the impact of the insertion time for the 0.6% Δk/k reactivity in the accident analysis. The time needed to eject the unsecured experiments from the core was conservatively set to 10 μs in the base case. In the Branch06b case the ejection time was increased to 0.1 seconds, which is a more realistic time. This adjustment reduces the accident consequence so that the peak fuel temperature in the limiting MOL plate is 0.9 °C lower than the base case.

The modeling variations in the Branch01, Branch03b, Branch04a, and Branch04b cases (shaded rows in Table 4) are either within the experimental uncertainty for the U-10Mo thermo-physical properties or within the allowed operations of the MURR. It is unlikely that the oxide layer thickness will increase by 23% relative to that predicted under the nominal operating conditions (Branch02), as that would require the reactor to operate consistently at the limits of the operating band. Among all of the cases considered, the peak U-10Mo fuel temperature was 270.9 °C for the accidental step insertion of 0.6% Δk/k in the LEU core ($0.78 inserted).

3.4 Conclusions

The insertion of excess reactivity in the HEU- and LEU-fueled MURR has been analyzed to assess the impact of a rapid step insertion of 0.6% Δk/k positive reactivity. This value is the MURR TS limit for the maximum allowed absolute reactivity worth of all unsecured experiments in the reactor. In the accident analyses, the modeling included depleted plates as well as fresh plates. Furthermore, a series of branch cases were modeled to cover potential non-conservative variations of thermo-physical properties or core operating conditions that may affect the severity of the accidents. No hot channel factors were applied in the reactivity insertion accident analyses.

The peak fuel temperature in the HEU cores for a rapid step insertion of 0.6% Δk/k positive reactivity always occurs in the fresh (BOL) plates. For the reference LEU cores with a mixture of elements at BOL, MOL, and EOL conditions, the peak fuel temperatures are in the depleted plates due to the degradation of the U-10Mo thermal conductivity with burnup, the growth of an oxide layer on the fuel plates during core residence, and the restriction of the coolant channel gap due to burnup effects (oxide layer, and fission-induced fuel swelling and creep).

In all of the HEU and LEU cases the fuel temperature remains well below temperatures where fuel blisters have been experimentally observed. In UAl_x fuel, blisters have been observed in the range of 480 to 598 ºC when irradiated fuel plates, at relevant fission densities, were placed in a furnace [16]. Only preliminary blister furnace data is available with monolithic UMo alloy fuel. For the monolithic UMo fuel blisters have been observed in the range of 400 to 530 ºC when irradiated fuel plates were placed in a furnace at fission densities relevant to MURR [17].

For the LEU MURR cores, EOL peak local fission density has been calculated to be between $1.1x10^{21}$ and $3.4x10^{21}$ fissions/cm^3 where the highest burnup is found in the outer plates of the element [14]. Monolithic UMo plates exceeding these burnup levels, up to $7x10^{21}$ fissions/cm^3, have been blister tested and exhibit a blister temperature no lower than 365 °C [17]. This preliminary UMo monolithic data was measured across a range of U-10Mo plate geometries, fabrication variables and irradiation conditions. Fuel plates specifically representative of MURR geometry and irradiation conditions will be blister annealed in future tests. Based on these preliminary measurements, there is significant margin between the temperature where blisters have been measured and the maximum fuel temperature calculated in the most limiting LEU reactivity insertion accident. Thus, the results of the analysis showed that the MURR can withstand these unexpected step reactivity insertions without damage to the fuel.

4. Loss of Coolant Accident

4.1 Introduction

Figure 1 provides a description of the MURR primary coolant system as it is represented in the simulation model. The solid red rectangle on the left side of the figure is the annular reactor core. Coolant flows downwards through the core to the lower plenum. From there the flow follows the piping that is shown in black through core outlet (hot-leg) isolation valve V507A and on to the primary coolant circulation pumps. In the coolant system there are two parallel pump

paths, each with its own pump and check valve. After the check valves, the two parallel paths rejoin for 7 feet (2 m) before dividing into two paths again, each with a heat exchanger followed by flow control diaphragm valve V540A or V540B. These two parallel paths then merge and follow a path to core inlet (cold-leg) isolation valve V507B and then through check valve V502 to the upper plenum, which connects to the top of the reactor core. In the model the two essentially identical parallel pump paths are combined into a single equivalent path, as are the two heat exchanger flow paths.

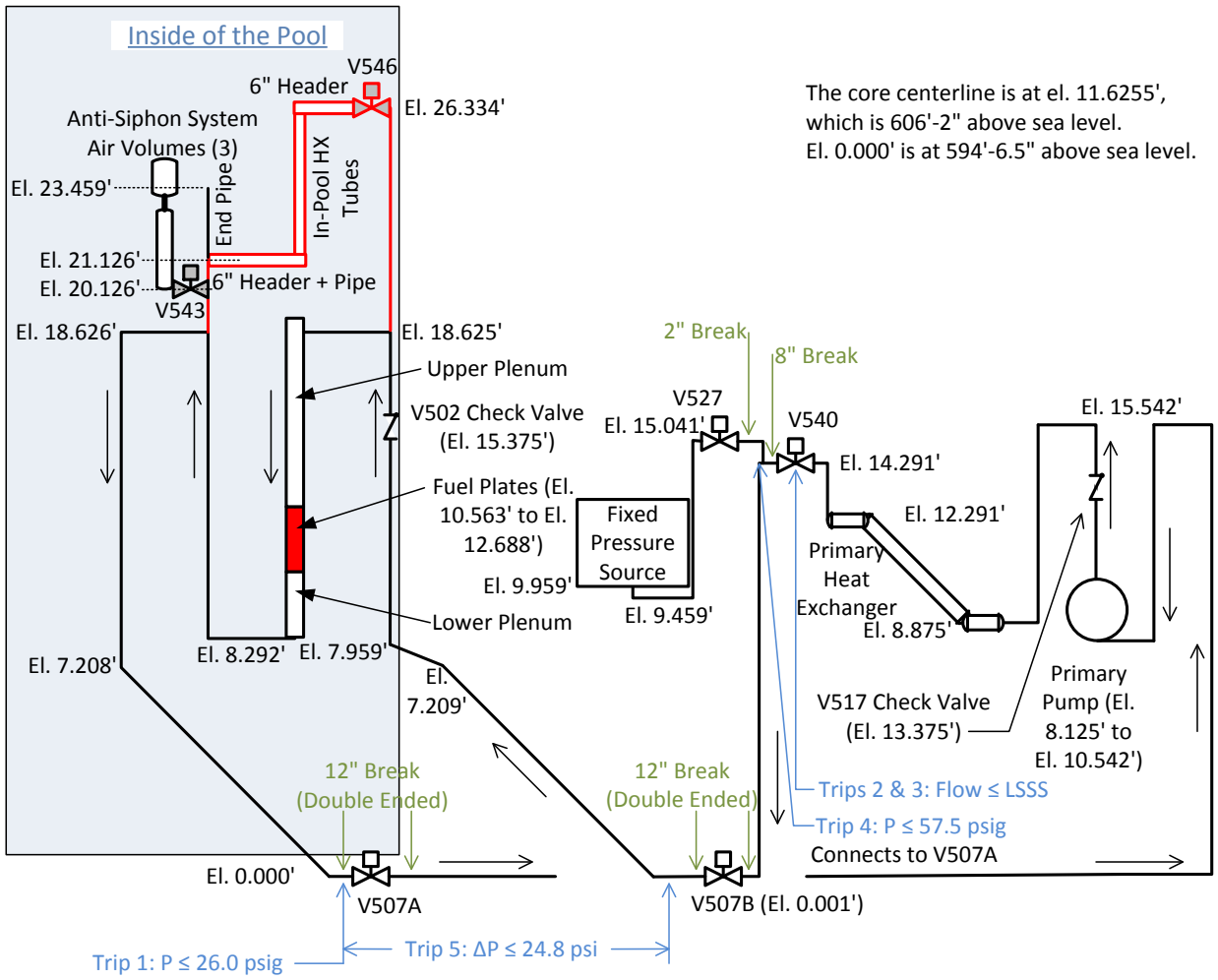

Figure 1 – RELAP5 Model of the MURR Primary Coolant System.

The upper plenum, reactor core, and lower plenum are contained within the pressurized reactor pressure vessels, which is not explicitly labeled in Figure 1. The shaded area in the figure labeled "Inside of the Pool" indicates the pool water, which surrounds the reactor pressure vessels and piping adjacent to the vessels. The surface of the pool is at atmospheric pressure, which is 14.3 psia (0.986 bar absolute). The pool water limits the loss of coolant during a primary loop breach that occurs within the pool boundary. Isolation valves V507A and V507B close during a Loss of Coolant Accident (LOCA) in order to minimize the loss of coolant from

the reactor pressure vessels. As Figure 1 shows, the piping exiting the lower plenum rises back up near the top of the pressure vessels before turning back downward. This piping arrangement is part of the overall design to minimize the loss of coolant from the reactor pressure vessels should the outlet piping break outside of the pool.

The pressurizer, as shown in the middle of Figure 1, is modeled as a fixed pressure source connected to the combined coolant flow path via a 2-inch (5.08 cm) line through isolation valve V527. In the actual primary coolant system, the pressurizer is attached via the 2-inch (5.08 cm) line to only one of the two paths. The initial pressure at this source is 78 psia (5.38 bar absolute).

A primary loop breach that occurs within the pool results in a depressurization and reactor scram and ejection of primary coolant from the pressurized system to the open pool. The six light green vertical arrows in Figure 1 indicate locations in the model where pipe breaks could occur. The primary loop breaches of greatest concern are the ones that occur outside of the pool between the biological shield and either of the two main isolation valves. Although not shown in the figure, at each arrow there is a fixed air pressure sink at atmospheric pressure of 14.3 psia that is separated from the pipe at that location by a closed valve whose full open diameter is that of the pipe in the system – 12, 8, or 2 inches (30, 20, or 5 cm) (All of these pipes are Schedule 40.). In a LOCA simulation one set of these closed valves is assumed to instantaneously go to its full open position, connecting the pipe to the adjacent fixed-pressure sink. The cold-leg LOCA caused by a double-end break at valve V507B is more severe than the hot-leg LOCA caused by a double-end break at valve V507A. This double-end break creates a sudden severe reduction in pressure upstream of the core, which produces a suction that immediately impedes core flow. A break upstream of valve V507A would tend to draw coolant flow towards the break and accelerate core flow, which helps cool the core. Thus, the cold-leg LOCA was found to be the most severe of the LOCAs.

Because all of these accidents are initiated by a depressurization of the primary coolant system, the automatic actions taken by the reactor protection systems are the same in each instance. A reactor scram is promptly initiated, the primary coolant circulation pumps trip, the two parallel redundant anti-siphon valves (V543 in Figure 1) open, the two main isolation valves (V507A and V507B) close, the two parallel redundant valves to the in-pool heat exchanger (V546 in Figure 1) open, and the pressurizer isolation valve V527C (V527 in Figure 1) closes. The reactor scram rapidly reduces reactor power to decay heat levels while the closing of valves V507A or V507B, and V527C minimize the loss of coolant.

The anti-siphon system contains compressed air that is injected into the top of the core outlet inverted loop by the opening of valves V543A and V543B (V543 in Figure 1). In the event of a hot-leg break immediately upstream of valve V507A, the injected air provides an air volume that expands and helps break any siphoning effect. Similarly, with check valve V502 on the primary coolant inlet piping riser, flow reversal of primary coolant is prevented, which eliminates any siphoning of the core from the cold-leg side of the reactor pressure vessels.

The in-pool heat exchanger is designed to facilitate decay heat removal from the core to the pool right after a scram from full-power operation. The system is designed so that when the main isolation valves are closed and the in-pool heat exchanger valves are open, water can circulate by

natural circulation between the core and the heat exchanger. Buoyancy causes the core flow direction to reverse. Heated coolant from the core flows upward and is cooled in the in-pool heat exchanger, which is located in the pool, and then flows downward and returns to the core via the reactor lower plenum. The air injected into the primary coolant loop by the anti-siphon system during a LOCA can collect at the top of the in-pool heat exchanger and severely impede or stop the natural circulation of water between the core and the in-pool heat exchanger. Thus, in a LOCA long-term decay heat removal is largely through the reactor pressure vessel walls.

Heat removal through the pressure vessel walls is enhanced by forced pool flow over the outer surfaces of the reactor pressure vessels, specifically in the control blade channels that surround the core and in the island tube at the core center. This flow is driven by the pool coolant circulation pump, which is not tripped as a result of a LOCA. The control blade channels do not extend significantly (~6 inches) above the core. Hence, virtually the entire outer convex surface of the reactor pressure vessel above the core is cooled by free convection from the vessel surface to the pool water. This free convection can be very effective in transferring decay heat to the pool water. Also, when there is no net flow through the reactor core, recirculation between the core coolant channels, with upward flow in the warmer channels and downward flow in the cooler channels, substantially facilitates heat removal.

During normal operation valves V546A and V546B (V546 in Figure 1), which are at the top of the in-pool heat exchanger, are closed and prevent flow through the heat exchanger, which is shown in red in Figure 1, and the primary coolant flow follows the path shown in black in the direction of the arrows.

4.2 Modeling

The RELAP5/MOD3.3 code [18] was used to represent the MURR primary coolant system as described in Figure 1. The core is comprised of eight (8) wedge-shaped 45° elements arranged to form an annular core with the inner pressure vessel providing space for the central flux trap. The total core (solid red rectangle in Figure 1) is represented as eight times the values of a single selected fuel element. In the model all of the element's coolant channels and fuel plates are explicitly represented. The azimuthal dimension of the coolant channel and fuel plate is increased by a factor of eight providing this same increase in the heat transfer area, coolant flow area, coolant flow rate, and power of each fuel plate, so that the one modeled element can take the place of all eight core elements.

All fresh HEU fuel elements are identical in design, as are all fresh LEU elements. However, burnup affects the thermal-hydraulic performance of the core by causing: 1) oxide to form on the fuel plate surfaces, 2) fuel meats to swell and, in turn, cause fuel plates to swell, and 3) fuel thermal conductivity to decrease. The oxide growth and fuel plate swelling restricts the coolant channels. Hence, in a core with elements of differing burnups, coolant is redistributed from the more burned elements to the less burned ones. In the RELAP5 model, the oxide layer, the reductions in coolant channels, and the reduction in fuel thermal conductivity are explicitly included.

Analysis showed the worst-case MURR cores consisted of two BOL fuel elements, four MOL elements (two pairs of slightly different burnups), and two EOL elements. The core flow rate for

the RELAP5 model was obtained from a separate hydraulics model that was evaluated via a computer spreadsheet. In the spreadsheet model the parallel channels of each pair of elements of the same burnup were modeled as a single flow path. The solution to this model provided a single flow rate for each pair of elements, which was assumed to be shared equally by both members of the pair.

In the RELAP5 model the initial primary coolant flow was taken to be eight times the flow rate of the element being modeled, as determined by the spreadsheet model. Each of the four parallel paths in the spreadsheet model was represented with a single combined flow area and a single hydraulic diameter. This hydraulic diameter was taken as four times the combined flow area of the path divided by the sum of all the wetted perimeters of all the coolant channels in the combined path.

Each fuel plate in the RELAP5 model was represented by only four nodes, which were stacked in the vertical direction. There are substantial variations in heat flux along the curved width of each fuel plate, i.e., in the azimuthal direction. In the separate neutronics calculations for the MURR cores, an azimuthal peak-to-average heat flux factor was determined for each fuel plate of each core. In the RELAP5 model the power of each fuel plate node was multiplied by its fuel plate azimuthal peak-to-average heat flux factor. The inclusion of these factors cause the power represented in the RELAP5 model to be considerably greater than what would be obtained with eight copies of the assumed limiting element. In the RELAP5 model of the BOL HEU core with the reactor operating at 10 MW, for example, 12.5 MW was used in the model. This accurately modeled the peak heat flux at each of the axial four nodes of the azimuthal hot strip of each fuel plate of the element being modeled, but caused a considerable increase in power represented in the model.

The initial reactor steady-state flow and temperature conditions for the RELAP5 model were taken to be the conservative ends of their normal operating bands. The normal operating primary coolant flow for the reactor is between 3700 and 3850 gpm (14.01 and 14.57 m^3/min). Therefore, in the separate spreadsheet model, 3700 gpm (14.01 m^3/min) was assumed and used to predict the initial flow rate for each core element. The normal operating core inlet temperature is between 118 and 125° F (48.8 and 51.7° C). Therefore, 125° F (51.7° C) was used for the initial steady-state conditions in the RELAP5 model. The maximum reactor power for the HEU core is 10 MW and 12 MW for the LEU core. Power measurement uncertainty is taken into account so that these values are not exceeded during the extremes of normal operation. Therefore, in the RELAP5 model, reactor power levels were set so that the heat flux at each fuel node corresponded to the azimuthal peak value for operating at 10 MW for the HEU core cases and 12 MW for the LEU core cases.

For the cold-leg LOCA the sequence of events is:

1. Double-ended break at isolation valve V507B (time = 0.0 s)
2. Rapid depressurization of the primary coolant system
3. Rapid reduction in core flow rate
4. Reactor scram (time = 0.325 s)
5. Peak fuel temperature reached (0.330 s $\leq$ time $\leq$ 0.340 s)

6. Primary coolant circulation pumps trip (time = 1.0 s)
7. Anti-siphon system injects air into the 12-inch (30-cm) core outlet piping (time = 1.0 s)
8. Main isolation valves V507A and V507B start closing at 4.5 s and are fully closed at 10 s
9. Core inlet check valve V502 closes to prevent coolant flow back towards the pipe break

4.3 Results

The RELAP5 model was used to determine the azimuthal hot stripe fuel centerline temperature histories for each of the four axial fuel nodes of each of the 24 fuel plates in the assumed limiting HEU element and for each of the 23 fuel plates of the assumed limiting LEU fuel element. Table 5 summarizes the peak fuel centerline temperatures for fuel elements at the BOL, MOL, and EOL for HEU Core 3A. The peak occurred in plate 1, which is the closest to the central flux trap, in the BOL and MOL elements, and in plate 2 in the EOL element. The initial steady-state temperature at the location of the peak is also provided in the table, along with the rise in temperature at that location from the steady-state to the peak value and the time after the break that the peak occurred. Analogous results are provided in Table 6 for LEU Core 7A. Here the limiting plate is plate 23, which is the outer most plate closest to the outer pressure vessel, for the BOL and MOL elements and is plate 22 for the EOL element. In every case the peak temperature occurred in the third axial fuel plate node of the four where the peak heat flux also occurs (the first node is at the top).

Table 5 shows that the peak HEU core temperature, 124° C, occurred in a BOL element. Table 6 shows that the peak LEU core temperature, 157° C, occurred in an EOL element. Figure 2 provides the peak temperature histories for these two elements. The initial rise in temperature from the steady-state condition is due to the rapid decrease in flow that is caused by the break, which occurs at time = 0. In both cases the reactor scram at 0.325 seconds causes the peak centerline time to decline shortly thereafter, at 0.340 seconds.

Table 5 – Loss of Coolant Accident Results - HEU Core.

Element Burnup	Initial Steady-State Temp., °C	Maximum Temp., °C	ΔT at Location of Max., °C	Time Max. Occurs, s
BOL, 0 MWd	108	**124**	16	0.340
MOL, 65 MWd	105	121	16	0.340
EOL, 150 MWd	99	114	15	0.340

Table 6 – Loss of Coolant Accident Results - LEU Core.

Element Burnup	Initial Steady-State Temp., °C	Maximum Temp., °C	ΔT at Location of Max., °C	Time Max. Occurs, s
BOL, 0 MWd	131	143	12	0.330
MOL, 96 MWd	141	153	12	0.330
EOL, 180 MWd	143	**157**	13	0.340

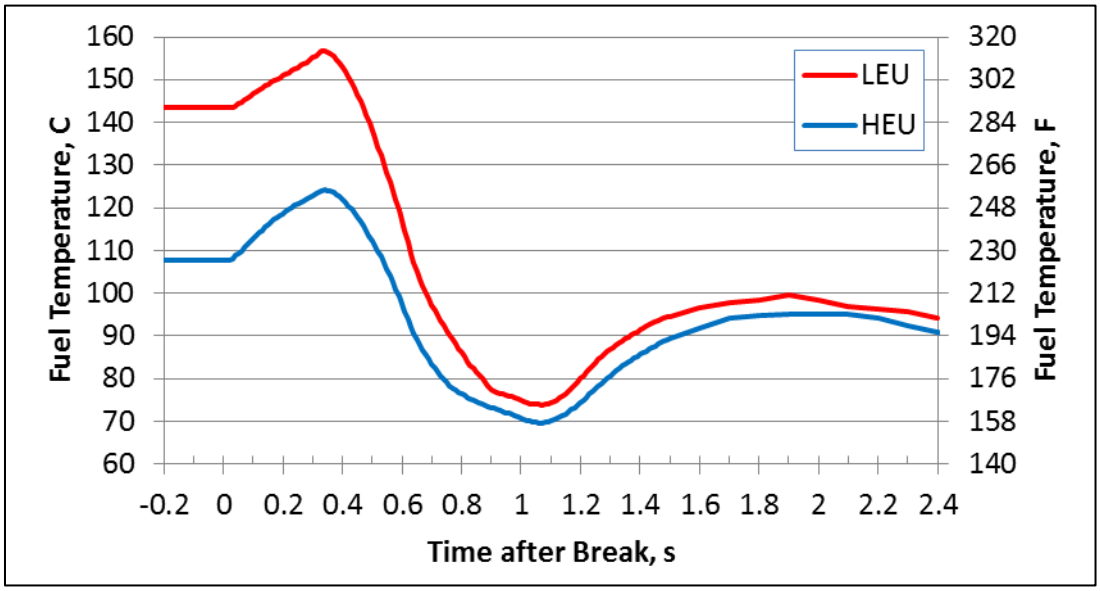

Figure 2 - LOCA Peak Fuel Centerline Temperature Histories at the Limiting Location.

4.4 Conclusions

The limiting large-break accident scenario for the MURR, the cold-leg LOCA caused by a double-end guillotine break of the main coolant inlet pipe immediately upstream of isolation valve V507B, has been analyzed for both HEU and LEU mixed-burnup cores. BOL, MOL and EOL fuel elements were considered. In the model, the axially varying heat flux distribution of each fuel plate of each fuel element has been multiplied by the plate's azimuthal peak-to-average heat flux ratio so that the model represents the peak heat flux at each axial level of each fuel plate at full plant operating power of 10 MW for the HEU core and 12 MW for LEU core. The transient simulations are initiated from the conservative end of the normal operating band for both reactor primary coolant flow and inlet temperature.

The peak fuel centerline temperature for the HEU core was found to be 124° C, which is only 16° C higher than the initial steady-state temperature at the same location in the core. Similarly, the peak fuel centerline temperature for the LEU core was found to be 157° C, which is only 13° C higher than the initial steady-state temperature at the same location in the core. Thus, the difference between the HEU and LEU peak fuel temperatures is largely or entirely due to the difference in initial steady-state fuel temperature.

In conclusion, for the limiting large-break accident scenario, both the HEU and the LEU core have a substantial margin to fuel damage.

5. Maximum Hypothetical Accident

5.1 Introduction

The analyses for the RIA and LOCA showed that no fuel damage is expected if these accidents were to occur. Consequently, there is no anticipated release of radioactive material as a result of these postulated accidents which would contribute a radiation dose to an individual inside (restricted area) or outside (unrestricted area) of the MURR facility. The Maximum Hypothetical Accident (MHA) postulates conditions leading to consequences worse than those from any credible accident. In the MHA for the MURR, it is assumed that some accident condition has caused fuel plates in the operating core to melt. The conditions that lead to this event are considered immaterial to the analysis. However, because of differences in the design and operating characteristics between the current HEU and the proposed LEU fuel elements, a different source term of radioactive material is considered in the accident analysis for the two cores. Specifically, the MHA for the HEU fuel assumes that four number-1 fuel plates in four separate elements melt. The number-1 plates are in the peak heat flux region of the HEU core. For the LEU core, the MHA assumes that four number-23 fuel plates in four separate elements melt. The number-23 fuel plates are in the peak heat flux region of the LEU core.

5.2 Methodology

The radioactive material source term for the MHA was calculated by assuming full-power operation in twelve 10-day cycles over a 300-day period. The HEU core power level is 10 MW, so that the fission product inventory in the core corresponds to a total core burnup of 1,200 MWd. This will give a conservative radioactive source term for the accident analysis, since the typical HEU core burnup in the MURR is only about 650 MWd. A fuel cycle simulation for the MURR operating with the proposed LEU fuel showed that the weekly operations cycle for the converted core will be the same as for the current HEU fuel [6]. Thus, the radioactive source term for the LEU core is still computed based on twelve 10-day cycles, but the core power level was increased to 12 MW. Consequently, the fission product inventory will correspond to a core burnup of 1,440 MWd, while the LEU core burnup in typical weekly operations is anticipated to be approximately 750 MWd.

The fission product inventory for the HEU core MHA analysis was originally calculated using the ORIGEN code [20, 21]. In this work however, due to better modeling and depletion simulation code packages (i.e., MONTEBURNS) [22], and the recent release of updated cross-section data [23], the fission products inventory calculations for the HEU core MHA was revised along with new fission products inventory calculation for the LEU core MHA.. The source term is based on the fraction of the whole core fission product inventory that is contained in the fuel plates that are damaged in the accident. For the HEU core, this fraction was calculated based on the fuel meat mass in the four number-1 plates that are assumed to melt and the power peaking factor in those plates. The number-1 plates are adjacent to the center flux trap. Reference 20 states that the four plates in the number-1 position comprise 1.3% of the fuel mass in the HEU core. A power peaking factor of 1.6 was applied to account for the fission rate and burnup of the number-1 plates, yielding 2.1% (1.3 x 1.6) as the fraction of the radioactive material in the whole core released in the MHA. The release of radioisotopes of krypton, xenon, and iodine are the

major sources of radiation exposure to personnel in the containment building and will, therefore, serve as the basis for the source term for the dose calculations. The source term for the LEU core can be calculated in a similar fashion to that done for the HEU core. The peak heat flux in the proposed LEU element occurs in plate number-23, which is adjacent to the beryllium reflector. Thus, the MHA will be analyzed assuming that four number-23 plates in the LEU core melt, which contain 2.72% of the fuel mass in the core. A radial power peaking factor of 2.01 for plate 23 was obtained from calculations performed in Reference 6 and applied to account for the fission rate and burnup of the number-23 plates, yielding 5.47% as the fraction of radioactive material in the whole core released in the MHA. Again, the radioisotopes of krypton, xenon, and iodine will serve as the basis of the source term.

The MHA is assumed to occur with the primary coolant system operating, resulting in a quick dispersal of all fission products in the melted fuel plates throughout the system. It is conservatively assumed that 100% of the radioiodine and noble gas fission products from the affected plates are instantaneously and uniformly dispersed within the 2,000-gallon (7,571 l) primary coolant system volume. The primary coolant system does experience some coolant leakage into the reactor pool, providing a path for personnel in the containment building to be exposed to radioactive material. This leakage is typically less than 40 gallons (151.4 l) per week. However, for the purpose of the MHA analysis, a conservative leakage rate of 80 gallons (302.8 l) per week (7.9×10^{-3} gpm or 3.0×10^{-2} lpm) from the primary coolant system to the pool was assumed.

5.3 Doses – Restricted Area

For calculating the occupational dose as a result of the MHA, it is assumed that personnel remain in the containment building for 10 minutes after the start of the accident, during which the staff would secure the primary coolant system and perform evacuation procedures. During this 10-minute interval, the radioiodines that transfer from the primary coolant system into the pool are conservatively assumed to instantaneously and uniformly mix into the 20,000 gallons (75,708 l) of bulk pool water. When the facility exhaust ventilation system is in operation, the evaporation rate from the reactor pool is approximately 80 gallons (302.8 l) of water per day (5.5×10^{-2} gpm or 2.1×10^{-1} lpm). For the purpose of the MHA, the assumption is that a total of 40 gallons (515.4 l) of pool water containing the radioiodines released from the fuel evaporates over 10 minutes into the containment building. The radioiodines are then assumed to uniformly mix into the containment building air volume of 225,000 ft^3 (6371.3 m^3). The noble gases (krypton and xenon) released from the primary coolant system over the 10 minute interval are assumed to pass immediately through the pool water and enter the containment building air volume. None of the assumptions related to the leakage rate of primary coolant to the pool, the pool evaporation rate, or the exposure time for personnel will be affected by the conversion to LEU fuel.

The objective of the analysis is to present a worst-case dose assessment for a person who remains in the containment building for 10 minutes following the MHA. Submersion in the airborne noble gas and iodine radionuclides inside the containment building will result in a whole-body radiation dose, as well as a thyroid dose from inhalation of the radioiodine. Decay of the radioisotopes is neglected in the analysis, so the calculated airborne concentration will increase linearly over the 10 minute interval. Therefore, the average concentrations of the noble gas and

iodine radionuclides for the dose calculations are best represented by the concentration existing at 5 minutes after the onset of the MHA. The external dose due to submersion is computed using the Derived Air Concentration (DAC) for radionuclides reported in Table 1 of Appendix B of 10 CFR 20 [24]. However, four radionuclides in the MHA source term do not have DAC values published in 10 CFR 20. These are ^{89}Kr, ^{90}Kr, ^{137}Xe, and ^{139}Xe. For these nuclides, DAC values equivalent to those utilized in the HEU MHA analysis [20] were employed.

Table 7 summarizes the results of the dose to personnel in the containment building (restricted area) calculated for the HEU and LEU MHA. The HEU results are from Reference 20. The doses resulting from the MHA in the LEU core are a factor of 3 to 4 higher than for the HEU core. This is because the assumed fraction of the core inventory contained in the damaged fuel plates is about a factor of 2.5 higher for the LEU core, and the 20% power uprate for the LEU core increases the core burnup and the whole core fission product inventory. The results in Table 7 show that the occupational doses are well within the published regulatory occupational limit of 5 rem for the total effective dose equivalent (TEDE) for both HEU and LEU cores.

Table 7 – 10-Minute Doses from Radioiodines and Noble Gases in Containment.

	HEU	**LEU**
Committed Dose Equivalent (CDE) to Thyroid, mrem	7.5	29.6
Committed Effective Dose Equivalent (CEDE) to Thyroid, mrem	0.23	0.889
Deep Dose Equivalent (DDE) from Radioiodines, mrem	0.052	0.16
Deep Dose Equivalent (DDE) from Noble Gases, mrem	132	407
Total Effective Dose Equivalent (TEDE) from Radioiodines, mrem	0.28	1.05
Total Effective Dose Equivalent (TEDE), mrem	132.28	408.05

If the default DAC values for ^{89}Kr, ^{90}Kr, ^{137}Xe, and ^{139}Xe from Table 1 of Appendix B of 10 CFR 20 are utilized in the dose calculations, the TEDE increases to 1,408 mrem. This dose is still below the regulatory limit of 5 rem published in 10 CFR 20. It is also worth noting that the expected evacuation time for most occupants of the containment building is around 2 minutes, instead of the 10 minutes assumed in the dose calculations. In that event, the dose will be a factor of 5 lower than the calculated values summarized above and in Table 7.

5.4 Doses – Unrestricted Area

It is highly probable that there will be no pressure differential between the inside of the containment building and the outside atmosphere, and consequently there will be no air leakage from the building and no radiation dose to members of the general public in the unrestricted area. Nonetheless, to develop what would clearly be a worst-case scenario, the MHA analysis assumes that there is some leakage of the air from the isolated containment building and the outside atmosphere. The assumption is made that an atmospheric pressure drop of 0.7 inches of Hg (0.33 psi) occurs at the onset of the MHA. The resulting pressure differential will result in an average leak rate of 5.2 scfm over a 16.5 hour period before the containment building pressure is equalized with the atmospheric pressure. Calculations were performed to compute the dose to individuals at various distances from the containment building during the entire 16.5 hour period

and under the most conservative (worst-case) meteorological conditions to obtain the maximum public dose.

The concentration of noble gas and iodine radionuclides in the containment building air can be calculated in the same manner as described in the previous section. It is further assumed that 100% of the noble gases in the containment air are released to the environment. However, experimental data have shown that 75% of the radioiodine in the containment air is deposited in the containment, so that only 25% of the radioiodine is released to the environment.

The point of maximum dose for a member of the general public in the unrestricted area was found to be 760 m north of the containment building. Table 8 summarizes the TEDE for the HEU and LEU MHA cases at that location. For the HEU MHA, the dose is taken from Reference20. In that analysis, the concentration of radioiodines and noble gases leaking from the containment was calculated at 10 minutes after the initiation of the MHA. The same approach was used for the LEU case, yielding a dose of 0.05 mrem. The dose calculation was also performed using the average concentration of radioiodines and noble gases in the containment over a 16.5 hour time period from the start of the MHA (i.e., the concentration at 8.25 hours). Because of the much longer time assumed for calculating the concentration of radioactive isotopes in the containment air, the calculated dose in the unrestricted area is about a factor of 50 greater (2.48 mrem vs. 0.05 mrem). Lastly, results were calculated using the unpublished DAC values from Table 1 of Appendix B of 10 CFR 20 for ^{89}Kr, ^{90}Kr, and ^{137}Xe, and ^{139}Xe, yielding a maximum dose of 8.61 mrem. Nonetheless, the calculated results show that the maximum dose is far below the applicable 10 CFR 20 regulatory limit of 2 mrem/hour for the unrestricted area.

Table 8 – Maximum Dose in the Unrestricted Area for 16.5 Hours Following the MHA.

		HEU	**LEU**		
			DACs from Reference 20		**DACs from Appendix B of 10 CFR 20**
Time from initiation of MHA at which concentration of radioiodines and noble gases leaking from containment are calculated.		10 minutes	10 minutes	8.25 hours (Average of 16.5 hours)	8.25 hours (Average of 16.5 hours)
TEDE	mrem	0.03	0.05	2.48	8.61
	mrem/hour	0	0	0.15	0.52

5.5 Conclusions

Dose to an individual in the restricted and unrestricted areas during an LEU core MHA have been calculated. Although the doses are higher during an LEU core MHA as compared to the HEU core MHA, they are still well within the regulatory limits of 10 CFR 20.

Acknowledgments

This work was supported by the U.S. Department of Energy, National Nuclear Security Administration Office of Global Threat Reduction.

References

[1] J. E. Matos and J. L. Snelgrove, "Selected Thermal Properties and Uranium Density Relations for Alloy, Aluminide, Oxide, and Silicide Fuel," *Research Reactor Core Conversion Guidebook*, IAEATECDOC-643, Volume 4: Fuels Appendices I-1.1, IAEA, Vienna, Austria, 1992, pp. 13-29.

[2] E. E. Feldman, et al., *Technical Basis in Support of the Conversion of the University of Missouri Research Reactor (MURR) Core from Highly-Enriched to Low-Enriched Uranium – Steady-State Thermal-Hydraulic Analysis*, ANL/RERTR/TM-12-37, Rev. 1, Argonne National Laboratory, January 2013.

[3] D. E. Burkes, G. S. Mickum, D. M. Wachs, *Thermophysical Properties of U-10Mo Alloy*, INL/EXT-10-19373, November 2010, Idaho National Laboratory.

[4] D. E. Burkes, et al, *Fuel Thermo-Physical Characterization Project: Fiscal Year 2013 Final Report*, PNNL-22981, November 2013.

[5] Burkes et al, "Thermo-Physical Properties of DU-10 wt.% Mo Alloys," *Journal of Nuclear Materials* (403, p. 160-166).

[6] J. Stillman, et al., *Technical Basis in Support of the Conversion of the University of Missouri Research Reactor (MURR) Core from High-Enriched to Low-Enriched Uranium – Core Neutron Physics*, ANL/RERTR/TM-12-30, Argonne National Laboratory, September 2012.

[7] *Department of Defense Handbook, Metallic Materials and Elements for Aerospace Vehicle Structures*, MIL-HDBK-5J, U. S. Department of Defense, January 31, 2003.

[8] J. K. Fink and L. Leibowitz, "Thermal Conductivity of Zirconium," *Journal of Materials*, 226 (1995) 44-50.

[9] J. C. Griess, H. C. Savage, and J. L. English, *Effect of Heat Flux on the Corrosion of Aluminum by Water. Part IV. Tests Relative to the Advanced Test Reactor and Correlation with Previous Results*, ORNL-3541, Oak Ridge National Laboratory, February 1964.

[10] *Guidelines for Preparing and Reviewing Applications for the Licensing of Non-Power Reactors, Standard Format and Content*, NUREG-1537, Part 1, February 1996.

[11] A. P. Olson, Argonne National Laboratory, unpublished information, 2014.

[12] X-5 Monte Carlo Team, "MCNP-A General Monte Carlo N-Particle Transport Code, Version 5 Volume I, II and III," LA-UR-03-1987/LA-CP-03-0245/LA-CP-03-0284, Los Alamos National Laboratory (2003).

[13] E. E. Feldman, et al, *Preliminary Accident Analyses for Conversion of the University of Missouri Research Reactor (MURR) from Highly-Enriched to Low-Enriched Uranium,* ANL/GTRI/TM-13/7, June 2013.

[14] J. A. Stillman et al, Irradiation Experiment Conceptual Design Parameters for MURR LEU U-Mo Fuel Conversion, ANL/GTRI/TM-13-1, Rev. 1, June 2013.

[15] M. Kalimullah, A.P. Olson, E.E. Feldman, N. Hanan and B. Dionne, *Verification and Validation of the PLTEMP/ANL Code for Thermal-Hydraulic Analysis of Experimental and Test Reactors*, ANL/RERTR/TM-11-37, Rev. 0, Nuclear Engineering Division, Argonne National Laboratory, Argonne, Illinois, July 30, 2011.

[16] J. M. Beeston, R. R. Hobbins, G. W. Gibson, and W. C. Francis, "Development and Irradiation of Uranium Aluminide Fuels in Test Reactors," *Nucl. Tech*., Vol. 49, p. 136-149 (June 1980).

[17] F. Rice, A. Robinson, M. Meyer, J. Fonnesbeck, D. Sell, P. Lind, and N. Lybeck "GTRI Blister Anneal and Fission Product Testing," U.S. High Performance Research Reactor Working Group Meeting, Los Alamos, New Mexico, June 11-13, 2013.

[18] The RELAP5/MOD3.3 Code Manual, Nuclear Systems Analysis Division, Information Systems Laboratories, Inc., Rockville, Maryland and Idaho Falls, Idaho, Prepared for the Division of Systems Research, Office of Nuclear Regulatory Research, U. S. Nuclear Regulatory Commission, Washington, DC 20555, March 2006.

[19] N. J. Peters, J.C. McKibben, K. Kutikkad, W.H. Miller, "Refining the Accuracy of Predicting Physics Parameters at Research Reactors due to the Limitations in Energy Balance Method using MCNP and the ENDF Evaluations", Nuclear Science and Engineering, 171(3): 210-219 (2012).

[20] *University of Missouri Research Reactor Safety Analysis Report*, submitted to the U.S. Nuclear Regulatory Commission in 2006.

[21] Bell, M. J., *ORIGEN – The ORNL Isotope Generation and Depletion Code*, Oak Ridge National Laboratory, ORNL-4628, May 1973.

[22] D. L. Poston, and H. R. Trellue, *User's Manual, Version 2.0 for MONTEBURNS Version 2.0*, LA-UR-99-4999, September 2002.

[23] M. B. Chadwick et al., "ENDF0B-VII.0: Next Generation Evaluated Nuclear Data Library for Nuclear Science and Technology," Nuclear Data Sheets, 107, 12, 2931 (2006).

[24] *NRC Regulations - Title 10, Code of Federal Regulations; Part 20: Standards for Protection Against Radiation*.